

Research Article

The Correlation between Pore Structure and Macro Durability Performance of Road Concrete under Loading and Freeze-Thaw and Drying-Wetting Cycles

Sheng-bo Zhou,¹ Jun-lin Liang,² Wei-an Xuan,¹ and Ye Qiu³

¹Guangxi Key Laboratory of Road Structure and Materials, Guangxi Transportation Research Institute Co., Ltd., Nanning 530007, China

²School of Civil Engineering & Architecture, Guangxi University, Nanning 530004, China

³College of Civil and Transportation Engineering, Hohai University, Nanjing 210098, China

Correspondence should be addressed to Jun-lin Liang; ljl_1217@126.com

Received 24 March 2017; Accepted 6 August 2017; Published 12 September 2017

Academic Editor: Xiao-Jian Gao

Copyright © 2017 Sheng-bo Zhou et al. This is an open access article distributed under the Creative Commons Attribution License, which permits unrestricted use, distribution, and reproduction in any medium, provided the original work is properly cited.

The grey correlation theory and multiple regression method are used to reveal macro performance degradation rules of road concrete under loading and freeze-thaw and drying-wetting cycles; then the correlation between mesoscopic pore structure and residual strength and antifreezing index of concrete is analyzed. Under the freeze-thaw and drying-wetting cycles with 50% loading level, the pore structure parameters that influence concrete strength show the following sequence: fractal dimension > most probable pore size > porosity > less harmful pore. The correlation between strength and pore parameters can be represented with multiple nonlinear equations. A negative correlation is shown between strength and fractal dimension and most probable pore size. Conversely, a positive correlation is shown between strength, porosity, and less harmful pore. Under the freeze-thaw and drying-wetting cycles with 80% loading level, the pore structure parameters that influence concrete strength show another sequence: fractal dimension > porosity > less harmful pore > most probable pore size. The correlation between antifreezing index and pore parameters should be described with multiple linear equations. The relative dynamic elastic modulus shows a positive correlation to most probable pore size, pore surface area, and porosity but a negative correlation to less harmful pore and pore spacing coefficient.

1. Introduction

Establishing the relationship between materials structure and performance has been a central content of materials science research. Professors Wu and Lian [1, 2] propose that the relation between different structure dimensions should be paid attention in research of concrete science and technology. Currently, scholars at home and abroad have carried out mechanical and durability research of concrete based on the mesostructure and microstructure level [3–8]. But the research achievement was rarely obtained about the relationship between pore structure and macro performance. So the fracture mechanics of concrete are urgent to be resolved. The destruction of road concrete is attributable to the interaction of loading and environment temperature-humidity. The

performance degradation of concrete would be accelerated when these factors alternate frequently. The failure condition of concrete in seasonal frozen area is studied in this paper. The relationship between mesostructure and macro performance is established which provides theoretical basis for concrete application and performance evaluation of this area.

The mesopore structure of concrete has a significant influence on the macro strength and antifreezing performance [9–12]. The pore structure is composed of several parameters, such as porosity, pore surface area, area median aperture, average aperture, most probable aperture, and pore fractal dimension. The concrete performance is affected by these parameters in different aspects and degrees [13–17]. In order to determine influence degree of every parameter and the main parameter, the grey system theory [18, 19] is needed

TABLE 1: Fatigue test conditions under loading and freeze-thaw and drying-wetting cycles.

Climatic region	Loading	Factors	
		Temperature and humidity	
		Winter	Summer
Alternating cold and drying-wetting region	50%; 80%	Temperature: $-18^{\circ}\text{C}\sim+5^{\circ}\text{C}$; humidity: 20%~40%	Temperature: $25^{\circ}\text{C}\sim35^{\circ}\text{C}$; humidity: 60%~80%

as traditional mathematical theory cannot be achieved. Grey correlation analysis is an effective system analysis method in grey system theory. It takes the uncertainty system with small sample and poor information as research object. After data processing, the main factors that influence research object would be found in random factors series. Therefore, it is especially suitable for the analysis of uncertain and complicated problems.

The basic steps of grey correlation analysis to deal with the problem are as follows.

(1) Determine reference sequence that reflects the behavior characteristics of system $X_i = \{x_i(k)|x_i(1), x_i(2), \dots, x_i(n)\}$, $i = 0, 1, 2, \dots, m$, and comparative sequence composed of each factor which affects system behavior $Y_i = \{y_i(k)|y_i(1), y_i(2), \dots, y_i(n)\}$, $i = 0, 1, 2, \dots, m$.

(2) In order to avoid the different data dimension as different physical meaning of each factor, make reference sequence and comparative sequence being dimensionless: $X'_i = \{x'_i(k)|x_i(1)/x_i(1), x_i(2)/x_i(1), \dots, x_i(n)/x_i(1)\}$, $i = 0, 1, 2, \dots, m$; $Y'_i = \{y'_i(k)|y_i(1)/y_i(1), y_i(2)/y_i(1), \dots, y_i(n)/y_i(1)\}$, $i = 0, 1, 2, \dots, m$. Calculate the difference sequence and range according to $\Delta_i(k) = |x_i(k) - y_i(k)|$. Then calculate grey correlation coefficient of reference sequence and comparative sequence based on $\gamma_i = (m + \xi M)/(\Delta_i(k) + \xi M)$, ($\xi = 0.5$); Finally calculate the correlation degree by $\gamma_{0i} = (1/n) \sum_{k=1}^n \gamma_i(k)$.

(3) Sort the correlation degree so as to reflect influence degree of each factor.

2. Test Scheme and Method

2.1. Test Scheme Design. The test loading is 50% and ultimate flexural loading is 80%, which correspond to ordinary traffic and heavy traffic levels. Freeze-thaw and drying-wetting cycles' environment mainly occurs in the temperate monsoon climate region: $-18^{\circ}\text{C}\sim+5^{\circ}\text{C}$ in winter and $25^{\circ}\text{C}\sim35^{\circ}\text{C}$ in summer. The relative humidity is 20%~40% in winter and 60%~80% in summer, which refers to the average humidity distribution given by Gao et al. [20] about five regions of Northeast China and North China, East China and Central China, Northwest China, South China, and Southwest China. The design conditions of concrete durability test under loading and freeze-thaw and drying-wetting cycles are shown in Table 1.

The test scheme is as follows.

First Stage. Firstly, the test beam is loaded 36 thousand times (50% stress level) or 12 thousand times (80% stress level) on the fatigue test machine. Then 50 freeze-thaw cycles (50% stress level) or 25 freeze-thaw cycles (80% stress level) at 4 hours intervals are conducted in environment box, with temperature range of $-18^{\circ}\text{C}\sim+5^{\circ}\text{C}$ and humidity range of 20%~40% with uniform rate. Take out the samples for second same loading and then place them in the environment box and reset temperature-humidity program: temperature range of $25^{\circ}\text{C}\sim35^{\circ}\text{C}$ and humidity range of 60%~80% with control interval at 4 h and a period of a month. At the end, the samples are taken out to test the strength, antifreezing index, and mesopore structure.

Second Stage. On the basis of the first stage, the cumulative test is conducted in accordance with the same procedure as the first phase. At the end, the samples are taken for the tensile strength test and mesostructure test.

Third Stage. On the basis of the second stage, fatigue loading was 18 thousand times (50% stress level) or 6 thousand times (80% stress level). Then 25 freeze-thaw cycles at 4 hours intervals are conducted in environment box under winter conditions. Take out the samples for the second 18 thousand times (50% stress level) or 6 thousand times (80% stress level) loading and then place them in the environment box and set the summer temperature-humidity conditions, with control interval at 4 h and a period of a month. At the end, the samples are taken for the above characterization test.

Fourth Stage. The test is conducted in accordance with the same procedure as the third phase until fatigue destruction. Then the samples are taken for the above characterization test.

2.2. Materials and Test Methods. Cement is Qinling P.O 42.5R; mineral filler is S95 class; fly ash is class I; coarse aggregate with nominal maximum size is 19 mm; fineness modulus of river sand is 2.6; water-reducing rate of high performance water reducer is 26%; water is tap water. 28 d concrete tensile design strength is C1, 4.5 MPa, and C2, 5.0 MPa.

The fatigue test is carried out on a 10 t MTS-810 fatigue testing machine; loading frequency is 10 HZ, loading mode is three-point sine wave, and low and high stress ratio is 0.1. Mesopore structure parameters are measured by AutoPore IV 9510 mercury porosimetry. Strength and antifreezing index test is in accordance with the specification.

3. Results Analysis and Discussion

3.1. Relationship between Pore Structure Parameters and Residual Flexural Strength under Loading and Freeze-Thaw and Drying-Wetting Cycles. The analysis result of grey correlation between pore structure parameters and residual flexural strength under different loading and freeze-thaw and drying-wetting cycles is obtained, as is shown in Table 2. It is known that, in the case of 50% loading level and freeze-thaw and drying-wetting cycles, the sequence of the correlation between pore structure parameters and residual flexural

TABLE 2: The grey correlation degree between pore structure parameters and strength under different loading levels and freeze-thaw and drying-wetting cycles.

Strength	Parameters					
	Porosity/%	Total pore surface area/m ² /g	Area median aperture/nm	Average aperture/nm	Most probable pore size/nm	Pore fractal dimension
50% loading						
C1	0.866	0.736	0.531	0.596	0.903	0.845
C2	0.889	0.749	0.549	0.538	0.893	0.850
80% loading						
C1	0.862	0.765	0.643	0.601	0.973	0.926
C2	0.886	0.728	0.670	0.575	0.909	0.910

Strength	Parameters					
	More harmful pore/nm	Harmful pore/nm	Less harmful pore/nm	Harmless pore/nm	Pore spacing coefficient	/
50% loading						
C1	0.777	0.627	0.858	0.815	0.716	/
C2	0.749	0.713	0.884	0.807	0.724	/
80% loading						
C1	0.856	0.771	0.915	0.823	0.843	/
C2	0.796	0.799	0.891	0.789	0.798	/

strength after three cycles is as follows: most probable pore size > porosity > less harmful pore > pore fractal dimension > harmless pore > more harmful pore > total pore surface area > pore spacing coefficient > harmful pore > area median aperture and average aperture. Results showed that the main pore structure parameters that influence the concrete strength are most probable pore size, porosity, less harmful pore, pore fractal dimension, and pore spacing coefficient. Similarly, in the case of 80% loading level and freeze-thaw and drying-wetting cycles, the sequence is as follows: most probable pore size > pore fractal dimension > less harmful pore > porosity > more harmful pore > pore spacing coefficient > harmless pore > harmful pore > total pore surface area > area median aperture and average aperture. The main pore structure parameters that influence the concrete strength are most probable pore size, pore fractal dimension, less harmful pore, porosity, and more harmful pore.

According to the results of grey correlation analysis, when establishing the relationship between strength and pore structure parameters under different loading and freeze-thaw and drying-wetting cycles, the four parameters of most

probable pore size, porosity, less harmful pore, and pore fractal dimension can be chosen as the main influencing factors. Formulas (1)~(4) are obtained by multiple linear regression analysis and multiple nonlinear regression analysis. When the loading level is 50%, a higher accuracy can be displayed using multiple nonlinear equation with the correlation coefficient of 0.970. A negative correlation is shown between strength and fractal dimension and most probable pore size. Conversely, a positive correlation is shown between strength and porosity and less harmful pore. The sequence according to influence degree is as follows: fractal dimension > most probable pore size > porosity > less harmful pore. When the loading level is 80%, the 0.999 correlation coefficient can be displayed, using both multiple linear equations and multiple nonlinear equations. A negative correlation is shown between strength and less harmful pore. Conversely, a positive correlation is shown between strength and fractal dimension, most probable pore size, and porosity. The sequence according to influence degree is as follows: fractal dimension > porosity > less harmful pore > most probable pore size.

$$\frac{\sigma}{\sigma_0} = 8.310 + 0.647 \times \frac{P_{lh}}{P_{lh0}} - 7.432 \times \frac{F_p}{F_{p0}} - 1.633 \times \frac{R_p}{R_{p0}} + 1.099 \times \frac{P_g}{P_{g0}} \quad (1)$$

(multiple linear regression at 50% loading levels, $R = 0.931$),

$$\frac{\sigma}{\sigma_0} = 0.977 \times \left(\frac{P_{lh}}{P_{lh0}}\right)^{0.986} \times \left(\frac{F_p}{F_{p0}}\right)^{-10.457} \times \left(\frac{I_p}{R_{p0}}\right)^{-2.637} \times \left(\frac{P_g}{P_{g0}}\right)^{1.036} \quad (2)$$

(multiple nonlinear regression at 50% loading levels, $R = 0.970$),

TABLE 3: Grey correlation degree between pore structure parameters and antifreezing index under different loading levels and freeze-thaw and drying-wetting cycles.

Strength	Parameters					
	Porosity/%	Total pore surface area/m ² /g	Area median aperture/nm	Average aperture/nm	Most probable pore size/nm	Pore fractal dimension
50% loading						
C1	0.905	0.838	0.533	0.585	0.782	0.733
C2	0.930	0.885	0.587	0.569	0.787	0.785
80% loading						
C1	0.842	0.896	0.579	0.561	0.749	0.731
C2	0.819	0.943	0.624	0.563	0.737	0.737

Strength	Parameters					
	More harmful pore/nm	Harmful pore/nm	Less harmful pore/nm	Harmless pore/nm	Pore spacing coefficient	/
50% loading						
C1	0.692	0.600	0.835	0.931	0.655	/
C2	0.710	0.699	0.807	0.957	0.704	/
80% loading						
C1	0.721	0.644	0.762	0.873	0.695	/
C2	0.690	0.700	0.739	0.900	0.691	/

$$\frac{\sigma}{\sigma_0} = 0.382 - 0.279 \times \frac{P_{lh}}{P_{lh0}} + 0.440 \times \frac{F_p}{F_{p0}} + 0.025 \times \frac{R_p}{R_{p0}} + 0.433 \times \frac{P_g}{P_{g0}} \quad (3)$$

(multiple linear regression at 80% loading levels, $R = 0.999$),

$$\frac{\sigma}{\sigma_0} = \left(\frac{P_{lh}}{P_{lh0}} \right)^{-0.701} \times \left(\frac{F_p}{F_{p0}} \right)^{-0.547} \times \left(\frac{R_p}{R_{p0}} \right)^{0.564} \times \left(\frac{P_g}{P_{g0}} \right)^{0.411} \quad (4)$$

(multiple nonlinear regression at 80% loading levels, $R = 0.999$).

3.2. Relationship between Pore Structure Parameters and Antifreezing Index under Loading, Freeze-Thaw, and Drying-Wetting Cycles. The analysis result of grey correlation between pore structure parameters and antifreezing index under different loading and freeze-thaw and drying-wetting cycles is shown in Table 3. The sequence of grey correlation degree is as follows: harmless pore > porosity > total pore surface area > less harmful pore > most probable pore size > pore fractal dimension > more harmful pore > pore spacing coefficient > harmful pore > area median aperture and average aperture, in the case of 50% loading level and freeze-thaw and drying-wetting cycles. Similarly, in the case of 80% loading level and freeze-thaw and drying-wetting cycles, the sequence is as follows: total pore surface area > harmless pore > porosity > less harmful pore > most probable pore size > pore fractal dimension > more harmful pore > harmful pore and average aperture > area median aperture > pore spacing coefficient.

According to the results of grey correlation analysis and considering the importance of less harmful pore and pore

spacing coefficient, when the relationship between antifreezing index and pore structure parameters is established under different loading and freeze-thaw and drying-wetting cycles, the five parameters, porosity, total pore surface area, less harmful pore, most probable pore size, and pore spacing coefficient, are chosen. Formulas (5)~(8) are obtained by regression analysis. Under these two loading levels and freeze-thaw and drying-wetting cycles, a higher accuracy can be displayed using multiple linear equation with the correlation coefficient of 0.999. The relative dynamic elastic modulus shows a positive correlation to most probable pore size, total pore surface area, and porosity but a negative correlation to less harmful pore and pore spacing coefficient. When the loading level is 50%, the sequence of pore structure parameters' influence on relative dynamic elastic modulus is as follows: pore spacing coefficient > total pore surface area > porosity > most probable pore size > less harmful pore. Meanwhile, when the loading level is 80%, the sequence is as follows: most probable pore size > porosity > pore spacing coefficient > less harmful pore > total pore surface area.

$$\frac{E}{E_0} = -0.336 + 0.291 \times \frac{R_p}{R_{p0}} + 0.336 \times \frac{S_g}{S_{g0}} - 0.048 \times \frac{P_{lh}}{P_{lh0}} + 0.296 \times \frac{P_g}{P_{g0}} - 0.365 \frac{L_p}{L_0} \quad (5)$$

(multiple linear regression at 50% loading levels, $R = 0.999$),

$$\frac{E}{E_0} = 0.998 \times \left(\frac{R_p}{R_{p0}}\right)^{0.146} \times \left(\frac{S_g}{S_{g0}}\right)^{0.267} \times \left(\frac{P_{lh}}{P_{lh0}}\right)^{-0.233} \times \left(\frac{P_g}{P_{g0}}\right)^{0.329} \times \left(\frac{L_p}{L_0}\right)^{-0.891} \quad (6)$$

(multiple nonlinear regression at 50% loading levels, $R = 0.985$),

$$\frac{E}{E_0} = -0.184 + 1.170 \times \frac{R_p}{R_{p0}} + 0.132 \times \frac{S_g}{S_{g0}} - 0.203 \times \frac{P_{lh}}{P_{lh0}} + 0.521 \times \frac{P_g}{P_{g0}} - 0.461 \frac{L_p}{L_0} \quad (7)$$

(multiple linear regression at 80% loading levels, $R = 0.999$),

$$\frac{E}{E_0} = \left(\frac{R_p}{R_{p0}}\right)^{4.612} \times \left(\frac{S_g}{S_{g0}}\right)^{0.058} \times \left(\frac{P_{lh}}{P_{lh0}}\right)^{-1.633} \times \left(\frac{P_g}{P_{g0}}\right)^{2.134} \times \left(\frac{L_p}{L_0}\right)^{-1.685} \quad (8)$$

(multiple nonlinear regression at 80% loading levels, $R = 0.998$).

4. Conclusion

(1) Under the ordinary traffic loading and freeze-thaw and drying-wetting cycles, the main pore structure parameters that influence concrete strength consist of most probable pore size, porosity, less harmful pore, pore fractal dimension, and pore spacing coefficient. Meanwhile, under the heavy traffic loading and freeze-thaw and drying-wetting cycles, the main pore structure parameters are most probable pore size, pore fractal dimension, less harmful pore, porosity, and more harmful pore. The reason is the stress concentration and stress diffusion process caused by superposition of multiple fields, along with the pore structure of the compression, and splitting effect occupied the leading position. The loading affects the pore size of the structure. As the loading level increased from 50% to 80%, the pore fractal dimension (pore complexity) has more influence on the stress diffusion than porosity. The amount of pore nucleation is only the inducing factor of the rapid development of concrete damage, but for the fracture of concrete under overloading, the effect of pore fractal dimension is more significant.

(2) Under the ordinary traffic loading and freeze-thaw and drying-wetting cycles, the correlation between strength and pore parameter should be represented with multiple nonlinear equation. A negative correlation is shown between strength and fractal dimension and most probable pore size. Conversely, a positive correlation is shown between strength and porosity and less harmful pore. The sequence according to influence degree is as follows: fractal dimension > most probable pore size > porosity > less harmful pore. Meanwhile, under the heavy traffic loading and freeze-thaw and drying-wetting cycles, a same high accuracy can be displayed using multiple linear equations and multiple nonlinear equations. A negative correlation is shown between strength and less harmful pore. Conversely, a positive correlation is shown between strength and fractal dimension, most probable pore

size, and porosity. The sequence according to influence degree is as follows: fractal dimension > porosity > less harmful pore > most probable pore size.

(3) Under freeze-thaw and drying-wetting cycles, under the ordinary traffic or heavy traffic loading, there is a higher correlation between antifreezing index and the five pore structure parameters: porosity, total pore surface area, less harmful pore, most probable pore size, and pore spacing coefficient.

(4) Under these two loading levels and freeze-thaw and drying-wetting cycles, the correlation between antifreezing index and pore parameters should be described with multiple linear equation. The relative dynamic elastic modulus shows a positive correlation to most probable pore size, total pore surface area, and porosity but a negative correlation to less harmful pore and pore spacing coefficient. Under the ordinary traffic, the sequence of pore structure parameters' influence on relative dynamic elastic modulus is as follows: pore spacing coefficient > total pore surface area > porosity > most probable pore size > less harmful pore. Meanwhile, under the heavy traffic, the sequence is as follows: most probable pore size > porosity > pore spacing coefficient > less harmful pore > total pore surface area.

Disclosure

Sheng-bo Zhou (1979-), Ph.D., senior engineer, mainly engaged in road cement concrete structure and material durability research; Jun-lin Liang, doctoral tutor, mainly engaged in highway engineering structural performance research.

Conflicts of Interest

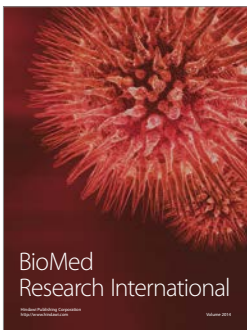
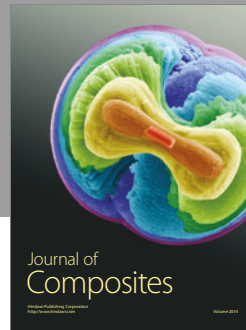
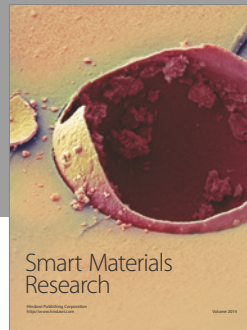
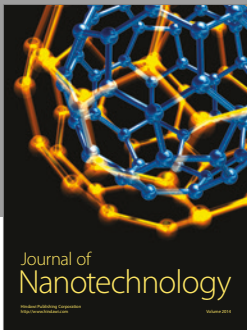
The authors declare that they have no conflicts of interest.

Acknowledgments

This research was supported by Guangxi Natural Science Foundation (Grant no. GUIKE AC16380109), the National Natural Science Foundation of China (51278059), and Opening Fund Project of Guangxi Key Lab of Road Structure and Materials (Project no. 2016gxjgclkf-004).

References

- [1] Z.-W. Wu, "Development prospects and problems of high performance concrete (HPC)," *Architecture Technology*, vol. 29, no. 1, pp. 8–13, 1998.
- [2] Z.-W. Wu and H.-Z. Lian, *High Performance Concrete*, China Railway Publishing House, Beijing, China, 1999.
- [3] P. K. Mehta and P. J. M. Monteiro, *Concrete Structure, Properties and Materials*, Prentice Hall, Upper Saddle River, NJ, USA, 1986.
- [4] M. Y. Du, X. Y. Jin, H. L. Ye, N. G. Jin, and Y. Tian, "A coupled hygro-thermal model of early-age concrete based on micro-pore structure evolution," *Construction and Building Materials*, vol. 111, pp. 689–698, 2016.
- [5] S. Goel, S. P. Singh, and P. Singh, "Flexural fatigue strength and failure probability of Self Compacting Fibre Reinforced Concrete beams," *Engineering Structures*, vol. 40, pp. 131–140, 2012.
- [6] J. Wawrzęczyk and W. Kozak, "Protected paste volume (PPV) as a parameter linking the air-pore structure in concrete with the frost resistance results," *Construction and Building Materials*, vol. 112, pp. 360–365, 2016.
- [7] X.-C. Pu and Y.-W. Wang, "Study on pore structure and interface structure of super high strength and high performance concrete," *China Concrete and Cement Products*, vol. 3, pp. 9–13, 2004.
- [8] W.-B. Xu, Z.-H. Shui, J.-T. Ma, and W. Chen, "Carbonation of Fly Ash Concrete Investigated with micro hardness analysis," *Bulletin of the Chinese Ceramic Society*, vol. 30, no. 1, pp. 7–12, 2011.
- [9] A. G. Graeff, K. Pilakoutas, K. Neocleous, and M. V. N. N. Peres, "Fatigue resistance and cracking mechanism of concrete pavements reinforced with recycled steel fibres recovered from post-consumer tyres," *Engineering Structures*, vol. 45, no. 10, pp. 385–395, 2012.
- [10] T. Matusinović, J. Šipušić, and N. Vrbos, "Porosity-strength relation in calcium aluminate cement pastes," *Cement and Concrete Research*, vol. 33, no. 11, pp. 1801–1806, 2003.
- [11] A. U. Ozturk and B. Baradan, "A comparison study of porosity and compressive strength mathematical models with image analysis," *Cement and Concrete Research*, vol. 43, no. 12, pp. 974–979, 2008.
- [12] I. Odler and M. Rossler, "Investigations on the relationship between porosity, structure and strength of hydrated Portland cement pastes II. Effect of pore structure and of degree of hydration," *Cement and Concrete Research*, vol. 15, no. 3, pp. 401–410, 1985.
- [13] R. Kumar and B. Bhattacharjee, "Porosity, pore size distribution and in situ strength of concrete," *Cement and Concrete Research*, vol. 33, no. 1, pp. 155–164, 2003.
- [14] X.-L. Zhao, J. Wei, and H.-J. Ba, "Relationship between frost durability and pore structure of high performance concrete," *Industrial Construction*, vol. 33, no. 8, pp. 5–27, 2003.
- [15] L. Chen, J.-H. He, and Y.-N. Zhao, "Relationship between pore structure of concrete and its frost durability degradation," *Communications Standardization*, vol. 2, pp. 70–75, 2009.
- [16] S.-P. Zhang, M. Deng, J.-H. Wu, and M.-S. Tang, "Effect of pore structure on the frost resistance of concrete," *Journal of Wuhan University of Technology*, vol. 30, no. 6, pp. 56–59, 2008.
- [17] Z. Giergiczny, M. A. Glinicki, M. Sokołowski, and M. Zielinski, "Air void system and frost-salt scaling of concrete containing slag-blended cement," *Construction and Building Materials*, vol. 23, no. 6, pp. 2451–2456, 2009.
- [18] J.-L. Deng, *Gray Prediction and Decision*, HuaZhong University of Science and Technology Publishing House, Wuhan, China, 1989.
- [19] M.-X. Jiang, *Grey Theory in the Study of Concrete Durability*, Nanjing University of Science & Technology, Nanjing, China, 2012.
- [20] H. Gao, N.-Q. Weng, G. Sun et al., "Distribution feature of meteorology parameter of upper air of different areas in China," *Journal of Atmospheric and Environmental Optics*, vol. 7, no. 2, pp. 101–107, 2012.



Hindawi

Submit your manuscripts at
<https://www.hindawi.com>

